Epsilon-Optimal Synthesis for Unicycle-like Vehicles with Limited Field-Of-View Sensors

Paolo Salaris, Andrea Cristofaro and Lucia Pallottino

***Abstract*—In this paper we study the minimum length paths covered by the center of a unicycle equipped with a limited Field–Of–View (FOV) camera, which must keep a given landmark in sight. Previous works on this subject have provided the optimal synthesis for the cases in which the FOV is only limited in the horizontal directions (i.e. left and right bounds) or in the vertical directions (i.e. upper and lower bounds). In this paper we show how to merge previous results and hence obtaining, for a realistic image plane modeled as a rectangle, a finite alphabet of extremal arcs and the overall synthesis. As shown, this objective can not be straightforwardly achieved from previous results but needs further analysis and developments. Moreover, there are initial configurations such that there exists no optimal path. Nonetheless, we are always able to provide an ε–optimal path whose length approximates arbitrarily well any other shorter path. As final results, we provide a partition of the motion plane in regions such that the optimal or ε–optimal path from each point in that region is univocally determined.**

I. Introduction

One of the most important issues in mobile robotics, which deeply influence the accomplishing of assigned tasks and hence the control laws, concern the directionality of motion (i.e. nonholonomic constraints) and sensory constraints (i.e. limited Field–Of–View (FOV) of cameras or scanners). For localization tasks or maintaining visibility of some objects in the environment, some landmarks must be kept in sight [1]. In visual servoing tasks, this problem becomes particularly noticeable and in the literature several solutions have been proposed to overcome it. However, when the FOV problem is successfully solved for a unicycle–like vehicle, as in [2], [3], the resultant path is not optimal.

Also in this paper, the problem of maintaining visibility (during all maneuvers and along all trajectories/paths) of a fixed landmark for a unicycle vehicle equipped with a camera with limited FOV is considered. The limited FOV problem is tackled here from an optimal point of view, i.e. finding shortest paths from any point on the motion plane to a desired configuration.

The problem addressed in this paper has also been studied in [4] and in [5]. Therefore, while in [4] only right and left camera limits, i.e. the Horizontal–FOV (H–FOV) constraints, were taken into account (see Fig. 1(a)), in [5] the complementary case with only upper and lower camera limits, i.e. the Vertical–FOV (V–FOV) constraints, is considered (see Fig. 1(b)). In the last case, the impracticality of paths that reach a compact set around the feature and the loss of geometrical properties of optimal arcs, lead to a substantially more complex analysis for the definition of the sufficient family of optimal paths with respect to the problem solved in [4]. Moreover, we proved that in some cases the optimal path does not exist. However, an ε–optimal path whose length approximates arbitrarily well any other shorter path has been obtained. Finally, in [6] a synthesis of shortest paths in case of lateral and side sensors (i.e. when the robot forward direction is not necessarily included inside the planar cone, cf. Fig. 1(a)), has been presented and includes, as a particular case, the synthesis provided in the earlier results [4].

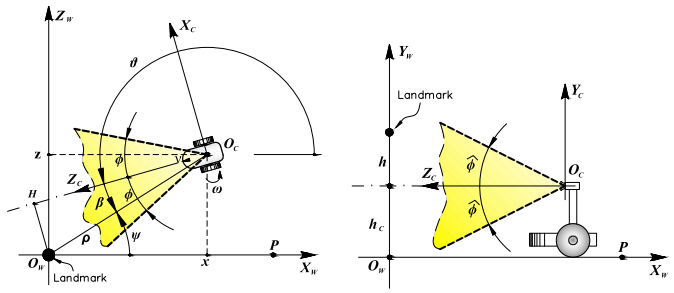

(a) Cartesian and polar coordinates of the robot w.r.t. world frame $\langle W \rangle$ and Horizontal–Field–of–View (H–FOV) constraints.

(b) Camera reference frame $\langle C \rangle$ and Vertical–Field–of–View (V–FOV) constraints.

Fig. 1: Mobile robot and systems coordinates. The robot's task is to reach P while keeping the landmark within a limited Field–of–View (dashed lines).

In this paper we describe how to merge results in [4] and in [5], obtaining, for the realistic case of FOVs modeled as a four–sided right rectangular pyramid (see Fig. 2) and an image plane modeled as a rectangle, a finite alphabet of extremal arcs from which an optimal path can be determined if any exists. Indeed, as in [5], we also show that in some cases there exists no optimal path. Moreover, we provide an ε–optimal path. Finally, we determine a partition of the motion plane in regions such that the optimal or ε–optimal path from each point in that region is univocally determined.

It is important to notice that, the objective of this paper can not be straightforwardly achieved from previous results but needs further analysis and developments. For example, we will show that, as in the V–FOV case, the shortest path may not exist and we provide conditions of existence. Furthermore, we will prove that paths of infimum length for the overall synthesis (HV–FOV synthesis) consist in subpaths that are of

This work was supported by E.C. n. 257462 HYCON2 (Network of Excellence) and n.2577649 PLANET.

Salaris is with INRIA, Sophia Antipolis, France. Cristofaro is with the Department of Engineering Cybernetics, Norwegian University of Science and Technology. Pallottino is with the Research Center "Enrico Piaggio" and Dipartimento di Ingegneria dell'Informazione, University of Pisa, Italy.

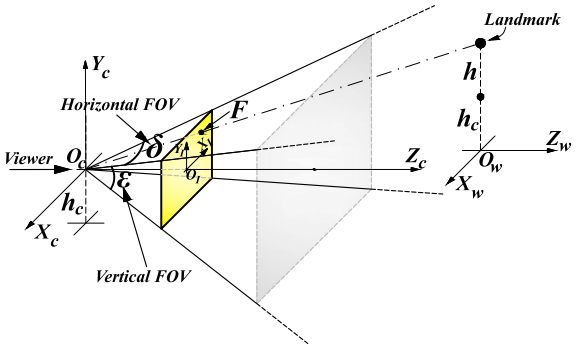

Fig. 2: Sensor model: four-sided right rectangular pyramid.

infimum length for the H–FOV and the V–FOV, respectively, and their conjunction is always smooth. Finally, we will show how considering all the involved constraints leads to paths of infimum length that were not present in the H–FOV and the V–FOV synthesis.

Regarding optimal (shortest) paths in absence of sensor constraints, the seminal work on unicycle vehicles, [7], provides a characterization of shortest curves for a car with a bounded turning radius. In [8], [9], authors determine a complete finite partition of the motion plane in regions characterizing the shortest path from all points in the same region, i.e. a synthesis. A similar problem with the car moving both forward and backward has been solved in [10] and refined in [11]. The global synthesis for the Reeds and Shepp vehicle has been obtained combining necessary conditions given by Pontryagin's Maximum Principle (PMP) with Lie algebraic tools in [12]. More recently, [13], [14] determined time optimal trajectories for differential–drive robots and nonholonomic bidirectional robots, respectively, while [15] solved the minimum wheel rotation problem for differential–drive robots.

The rest of the paper is organized as follows: first the optimal control problem is introduced (Section II) with the analysis of constraints and the characterization of the extremal arcs. In Section III the main results obtained in [4] and in [5], necessary to obtain the complete HV–FOV synthesis, are reported. The characterization of the extremal concatenations in optimal paths is also addressed obtaining a finite family of optimal concatenations summarized in the ε-optimal graph. In Section IV and V the complete HV–FOV synthesis is obtained for particular ranges of values of significant parameters. HV–FOV synthesis for different values of those parameters are reported in the with some other minor and technical results in the Technical Report [16].

II. Problem Definition

Consider a vehicle moving on a plane where a right-handed reference frame $\langle W \rangle$ is defined with origin in O_w and axes X_w, Z_w. The configuration of the vehicle is described by $\xi(t) = (x(t), z(t), \theta(t))$, where $(x(t), z(t))$ is the position in $\langle W \rangle$ of a reference point in the vehicle, and $\theta(t)$ is the vehicle heading with respect to the X_w axis (see Fig. 1). We assume that the dynamics of the vehicle are negligible, and that linear and angular velocities, $v(t)$ and $\omega(t)$ respectively, are the control inputs of the kinematic model of the vehicle. Choosing polar coordinates (see Fig. 1), the kinematic model of the unicycle-like robot is

$$\begin{bmatrix} \dot{\rho} \\ \dot{\psi} \\ \dot{\beta} \end{bmatrix} = \begin{bmatrix} -\cos\beta & 0 \\ \frac{\sin\beta}{\rho} & 0 \\ \frac{\sin\beta}{\rho} & -1 \end{bmatrix} \begin{bmatrix} v \\ \omega \end{bmatrix}. \tag{1}$$

We consider vehicles with bounded velocities which can turn on the spot. In other words, we assume

$$(v, \omega) \in U, \tag{2}$$

with U a compact and convex subset of $\mathbb{R}^2$, containing the origin in its interior.

The vehicle is equipped with a rigidly fixed pinhole camera with a reference frame $\langle C \rangle = \{O_c, X_c, Y_c, Z_c\}$ such that the optical center O_c corresponds to the robot's center $[x(t), z(t)]^T$ and the optical axis Z_c is aligned with the robot's forward direction. Pinhole cameras can be modeled as a four-sided right rectangular pyramid, as shown in Fig. 2. Its characteristic solid angle is given by $\Omega = 4 \arcsin\left(\sin\frac{\varepsilon}{2}\sin\frac{\delta}{2}\right)$, where $\varepsilon = 2\hat{\phi}$ and $\delta = 2\phi$ are the apex angles, i.e. dihedral angles measured to the opposite side faces of the pyramid. We will refer to those angles as the vertical and horizontal angular aperture of the sensor, respectively. Moreover, $\hat{\phi}$ is half of the V–FOV angular aperture, whereas ϕ is half of the H–FOV angular aperture. In the following, we consider the most interesting case in which ε and δ are less than π.

We assume that the feature to be kept within the on-board limited FOV sensor is placed on the axis through the origin O_w, perpendicular to the plane of motion, so that its projection on the motion plane coincides with the center O_w (see Fig. 1). The feature has height $h + h_c$ from O_w and height h from the plane $X_c \times Z_c$ (see Fig. 2). Moreover, let us consider the position of the robot target point P to lay on the X_w axis, with coordinates $(\rho, \psi) = (\rho_P, 0)$. In order to maintain the feature within the limited FOV sensor, the following inequality constraints must be satisfied during robot's maneuvers:

$$\beta + \phi \geq 0, \tag{3}$$

$$\beta - \phi \leq 0, \tag{4}$$

$$\rho\cos\beta \geq \frac{h}{\tan\hat{\phi}} = R_b. \tag{5}$$

Inequalities (3) and (4) concern H–FOV limits (see [4] for details) whereas inequality (5) concerns V–FOV limits (see [5] for details).

A. Analysis of FOV Constraints

In this subsection we analyze the FOV constraints (3), (4) and (5). In particular, we will show that the H–FOV constraints and the V–FOV constraint can not be simultaneously activated apart from on a circle centered in O_W and with radius $R_b/\cos\phi$. Let us preliminary state the following

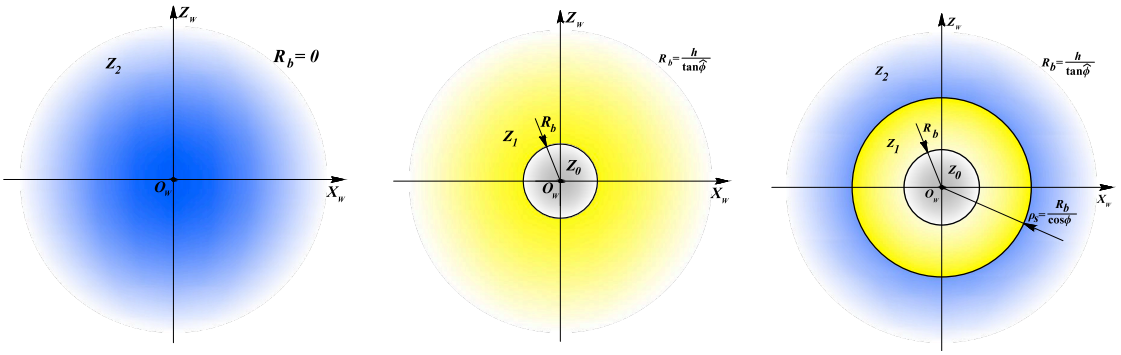

(a) Subdivision of the motion plane in case of only the H–FOV constraints are considered, as in [4].

(b) Subdivision of the motion plane in case of only the V–FOV constraint is considered, as in [5].

(c) Subdivision of the motion plane according to Remark 1, when both the H–FOV and the V–FOV constraints are considered.

Fig. 3: Subdivision of the motion plane according to Remark 1 and the particular cases in which no restriction on vertical or horizontal FOV is assumed.

Definition 1: Let $Z_0 = \{(\rho, \psi) | \rho < R_b\}$ be the disk centered in the origin with radius R_b, $Z_1 = \{(\rho, \psi) | R_b \leq \rho \leq \frac{R_b}{\cos\phi}\}$, $Z_2 = \{(\rho, \psi) | \rho > \frac{R_b}{\cos\phi}\}$ and C_S the circumference with radius $\rho_S = R_b / \cos\phi$.

Remark 1: Referring to Fig. 3(c), Z_0 is the set of points in $\mathbb{R}^2$ that violate the V–FOV constraint (5) for any value of β. Notice that points with $\rho = R_b$ verify the constraint only if $\beta = 0$. It is straightforward to notice that points in Z_1 that verify, as an equality, one of the H–FOV constraints, violate the V–FOV constraint. Only for points on C_S both constraints are verified as an equality, i.e. for $\rho = \rho_S$ and $\beta = \pm\phi$. On the other hand, points in Z_1 that verify the V–FOV constraint do always verify both H–FOV ones. Hence, for points in Z_1 the H–FOV constraints are verified for points that verify the V–FOV one while the vice–versa is not true. Moreover, it is straightforward to notice that points in Z_2 that verify the V–FOV constraint, as an equality, violate both H–FOV ones. On the other hand, points in Z_2 that verify both the H–FOV constraints do always verify the V–FOV one. Hence, for points in Z_2 the V–FOV constraint is verified for points that verify both H–FOV ones while the reverse is not true.

An important consequence of Remark 1 is that the H–FOV constraint (4) (or (3)) and the V–FOV one (5) are concurrently activated, i.e. they hold as equality with $\beta = \phi$ (or $\beta = -\phi$), $\rho = \rho_S$. Moreover, in Z_1 the V–FOV constraint is more restrictive than the H–FOV ones while the opposite holds in Z_2.

B. Optimal Control Problem and Extremal Arcs

The goal of this paper is to determine, for any point $Q \in \mathbb{R}^2$ in the motion plane, the minimum length path covered by the center of the vehicle from Q to P, such that the landmark is always maintained in the FOV of the sensor during maneuvers. In other words, the objective is to minimize the cost functional

$$L = \int_0^\tau |v| \, dt \,, \tag{6}$$

under the *feasibility constraints* (1), (2) (3), (4) and (5), respectively. Here τ is the time needed to reach P, that is without loss of generality, $\rho(\tau) = \rho_P$ and $\psi(\tau) = 0$.

Previous analysis and consequent results suggest that a solution to this problem can be accomplished by preliminary solving two sub–problems in which only the H–FOV or the V–FOV constraints are taken into account. These two sub–problems have been already solved in [4] and [5]. In the first case the vertical aperture is π, i.e. $\hat{\phi} = \pi/2$ and hence $R_b = \rho_S = 0$. As a consequence, Z_0 and Z_1 degenerate in O_W, and $Z_2 \equiv \mathbb{R}^2$, i.e. the subdivision of Fig. 3(c) becomes as in Fig. 3(a). In [4], it has been proved that the optimal paths consists of at most 5 arcs of three types: rotations on the spot (denoted by the symbol $*$), straight lines (denoted by the symbol S) and left and right logarithmic spirals (denoted by symbols T^L and T^R) of characteristic angle ϕ. In the second sub–problem, the horizontal camera aperture is π, i.e. $\phi = \pi/2$, and hence $\rho_S \to \infty$. As a consequence, the subdivision of Fig. 3(c) becomes as in Fig. 3(b). In [5] it has been shown that the optimal paths consist of at most 5 arcs of three types: rotation on the spot ($*$), straight lines (S) and left and right involute of circles (denoted by symbols I^L and I^R).

For the overall problem considered in this paper, we have hence six extremal arcs, represented by $\{*, S, T^R, T^L, I^R, I^L\}$. Rotations on the spot have zero length but are used to properly connect the other arcs. Of course, extremals can be executed in either forward or backward directions. Hence, by using superscripts $+$ and $-$ to make this explicit, extremal paths will consist of a sequence, or *word*, in the alphabet $\{*, S^-, S^+, T^{R+}, T^{R-}, T^{L+}, T^{L-}, I^{R+}, I^{R-}, I^{L+}, I^{L-}\}$. All the possible words generated by the above alphabet forms a language $\mathscr{L}$. The first goal of this paper is to determine

under which conditions there exists a sufficient finite optimal language such that, for any initial configuration, it contains a word describing a path to the goal which is no longer than any other feasible path.

Remark 2: From the optimality principle, even if previous works provide the H–FOV synthesis and the V–FOV synthesis, a solution for the HV–FOV synthesis can not be obtained simply from those solutions, i.e. concatenation of two optimal path is not necessarily optimal. Of course, there are some regions of the HV–FOV synthesis entirely inherited from the V–FOV synthesis and the H–FOV synthesis, i.e. regions of points such that the path from Q to P does not intersect C_S, refer to Section IV. On the other hand, for all paths that cross the boundary between Z_1 and Z_2 an analysis on how the extremals are concatenated across C_S must be achieved (cf. Section III-C).

III. Analysis of extremals concatenations

The goal of this section is to characterize the family of optimal extremals concatenations. As in the case of H–FOV and V–FOV analysis, the first step is to reduce the complexity of the problem by excluding possible combinations of extremal arcs in the optimal path, hence obtaining, at the end of this section, a finite family of extremals concatenations.

After summarizing the main results of previous papers [4] and [5] that will be useful also in this analysis, we will provide the optimality conditions for paths crossing the border C_S between Regions Z_1 and Z_2. We will show that in any optimal path the extremals are tangent one to another in points of C_S (Subsection III-C). We will then provide the optimality condition of paths that cross the circumference C_S at least twice before reaching P (Subsection III-D).

A. From H–FOV and V–FOV synthesis: basic definitions and results

For the reader convenience, we first recall the basic concepts already introduced in [4] and in [5], for the H–FOV and the V–FOV respectively, and that will be useful also in this analysis. Let $\mathscr{P}_Q \in \mathscr{L}$ be the set of all feasible extremal paths from Q to P. In the rest of the paper we will study which combination of extremals belongs to the optimal path in $\mathscr{P}_Q$.

Due to the symmetry of the problem, the analysis of optimal paths in $\mathscr{P}_Q$ can be done considering only points Q in the upper half plane w.r.t. the X_w axis.

Definition 2: An extremal path in $\mathscr{P}_Q$, described by a word $w \in \mathscr{L}$ is a *palindrome symmetric path* if the word is palindrome and the path is symmetric w.r.t. the bisectrix of angle $\widehat{QO_wP}$.

We recall that a word is palindrome if it reads equally forward or backward. As an example, the path $S^+T^{L+} * T^{R-}S^-$ is a palindrome symmetric path, associated to the palindrome word $STTS$, if the straight arcs and the spiral arcs are of equal length pairwise.

Let CP be the circumference centered in O_W with radius ρ_P, DS be the closure of the semi-disk in the upper-half plane and CS its semicircle.

Proposition 1: For any path in $\mathscr{P}_Q$ from $Q \in CP$ there always exists a palindrome symmetric path in $\mathscr{P}_Q$ whose length is shorter or equal.

The proof of proposition 1 can be found in [4] for the H–FOV synthesis and in [5] for the V–FOV synthesis.

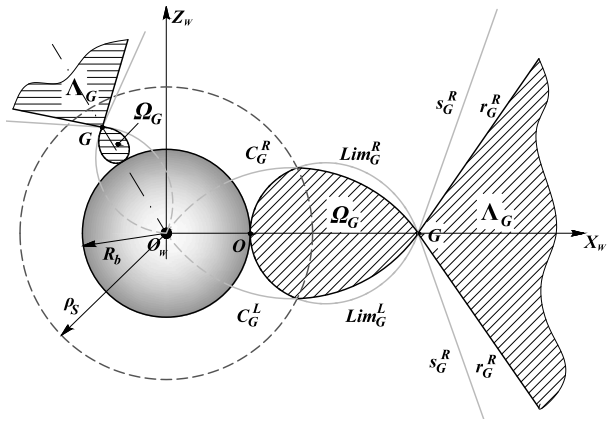

Fig. 4: Borders and regions from which the optimal path is a straight line for the H–FOV (i.e. C_G^R, C_G^L, r_G^R and r_G^L) and the V–FOV (i.e. Lim_G^R, Lim_G^L, s_G^R and s_G^L) cases, separately. Moreover, for points $G \in Z_2$, i.e. $\rho_G > \rho_S$, any point inside $\Omega_G = Lim_G \cap C_G$ (Λ_G with apex angle 2ϕ) can be reached by S^+ (S^-) (see Proposition 2), i.e. Ω_G and Λ_G are the regions from which the optimal path is a straight line for the HV–FOV case. In case of $G \in Z_1$, i.e. $R_b \le \rho_G \le \rho_S$ Region Ω_G coincides with Lim_G while the region of points reachable by S^- is a cone Λ_G with apex angle $\tilde{\beta}$. $\tilde{\beta}$ is zero when $\rho_G = R_b$ and it is equal to ϕ when $\rho_G = \frac{R_b}{\cos\phi} = \rho_S$.

The following definitions and remarks recall the terminology used for the H–FOV and the V–FOV, to indicate borders of regions whose optimal paths consist only of a straight line.

Definition 3: For a point $G \in \mathbb{R}^2$, let C_G^R (C_G^L) denote the circular arc from G to O_w such that, $\forall V \in C_G^R$ (C_G^L), $\widehat{GVO_w} = \pi - \phi$ in the half-plane on the right (left) of $\overline{GO_w}$ (cf. Fig. 4). In addition, let C_G denote the region delimited by C_G^R and C_G^L from G to O_w.

Definition 4: For a point $G \in \mathbb{R}^2$, let Lim_G^R (Lim_G^L) denote the arc of the Limaçon from G to O such that, $\forall V \in Lim_G^R$ (Lim_G^L), $\widehat{GVO_w} = \pi - \tilde{\beta}$, with $\tilde{\beta} = \arctan\left(\frac{\rho_G}{Rb}\sin\beta\right)$, in the half-plane on the right (left) of $\overline{GO_w}$ (cf. Fig. 4). Also, let Lim_G denote the region delimited by Lim_G^R and Lim_G^L from G to O.

In [4] ([5]) it has been proved that C_G (Lim_G) is the region of points from which G can be reached with an arc S^- without violating the H–FOV (V–FOV) constraints. Moreover, we denote their intersection as $\Omega_G = Lim_G \cap C_G$.

Definition 5: For a point $G \in \mathbb{R}^2$, let s_G^R (s_G^L) denote the half–line from G forming an angle $\psi_G + \tilde{\beta}$ ($\psi_G - \tilde{\beta}$) with the X_w axis (cf. Fig. 4) where $\tilde{\beta} = \arccos\frac{R_b}{\rho_G}$. In addition, let Λ_G denote the cone delimited by s_G^R and s_G^L.

If $G \in Z_2$, $\tilde{\beta} \equiv \phi$ and half–lines s_G^R, s_G^L are denoted with r_G^R, r_G^L. In [4] and [5] it has been proved that Λ_G is the region

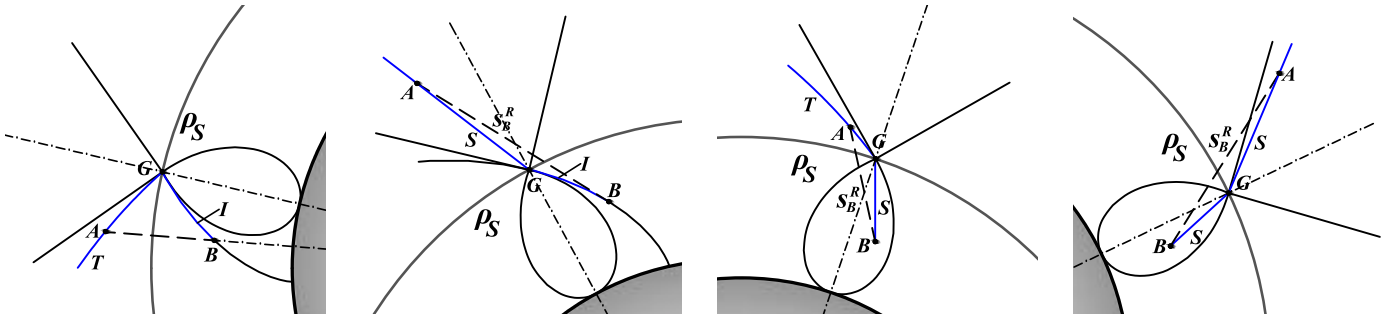

(a) Path of type $T^L * I^R$. (b) Path of type $S * I$. (c) Path of type $T * S$. (d) Path of type $S * S$.

Fig. 5: Any optimal path that crosses circumference C_S in G is smooth in G.

of points from which G can be reached with an arc S^+ without violating any of the H–FOV and the V–FOV constraints.

Remark 3: For $G \in Z_1$ the apex angle of cone Λ_G increases with $R_b \leq \rho_G \leq \rho_S$ up to 2ϕ when $G \in C_S$.

Remark 4: It is worth noting that from the definitions above, the straight arc S between two points $A, B \in Z_1 \cup Z_2$ with $\psi_A = \psi_B$, i.e. aligned with O_W, never violates neither the H–FOV constraints nor the V–FOV one.

Finally, from results reported in [5] on the analysis of the V–FOV case, let us introduce circumferences C_2 and C_5 with radii $\rho_2 = R_b\sqrt{2}$ and $\rho_5 = R_b\sqrt{5}$, respectively. In particular, the resulting V–FOV optimal synthesis deeply depends on the position of the final and initial points P and Q, respectively, w.r.t. C_2 and C_5. Similarly, as shown in next sections, these two circumferences play an important role also for the HV–FOV synthesis.

B. Straight line regions for the HV–FOV synthesis

As a first step toward the HV–FOV synthesis, we first study the regions of points that can be reached, starting from a point G, through a straight line, i.e. paths of type S^+ or S^-. Referring to Fig. 4, in case of both the H–FOV and the V–FOV constraints we have:

Proposition 2: For any starting point $G \in Z_1 \cup Z_2$, all points of $\Omega_G = Lim_G \cap C_G$ (Λ_G) are reachable by a forward (backward) straight path without violating neither the V–FOV nor the H–FOV constraints.

The proof follows straightforwardly from the results in [4] and [5] summarized in previous subsection and simple geometric considerations.

C. Smoothness of optimal concatenations across C_S

To compute the optimal synthesis, we first need to analyze how to optimally connect the synthesis provided in [4] and [5], i.e. how optimal paths toward P may cross circumference C_S.

As shown in [5], optimal paths may not exist. In such cases, the path of infimum (finite) length has been proved to consist of infinite switches on C_2. In this section we will show that also for the HV–FOV synthesis there are initial and final configurations such that the optimal path does not exist and the infimum path length consists of infinite switches on C_2 or C_S depending on the value of ϕ and $\hat{\phi}$.

Let us start considering how to optimally connect, on C_S, extremals $E_1 = \{S, T^R, T^L\}$ related to the H–FOV constraints with extremals $E_2 = \{S, I^R, I^L\}$ related to the V–FOV constraint.

Proposition 3: In any optimal path, extremal arcs in E_1 are tangent on C_S to extremal arcs in E_2.

Proof: Without loss of generality we consider a path γ that starts outside C_S and intersects it in G. The possible combinations of non tangent extremals (in G) for γ with switching point G are: $S * S$, $S * I$, $T * S$ and $T * I$. We will refer to such concatenations between arcs in E_1 and E_2 as non smooth concatenations on C_S.

The concatenation of two left (or right) arcs, i.e. T^L and I^L (or T^R and I^R), with intersection point $G \in C_S$ is smooth in G since $\beta_G = -\phi$ (or $\beta_G = \phi$) for both arcs T and I and hence arcs T and I are tangent on C_S. Referring to Fig. 5(a), concatenations of type $T^L * I^R$ and $T^R * I^L$ can always be shortened with straight segments across C_S since there exist points A on T and B on I such that $\psi_A = \psi_B$ and since from Remark 4 the segment $\overline{AB}$ does not violate the constraints.

Referring to Figures 5(b), 5(c) and 5(d), consider now a concatenation $E_2 * E_1$ of type $S * I$, $T * S$ and $S * S$ respectively. There always exist points $A \in Z_2$ on E_2 and $B \in Z_1$ on E_1 such that $A \in \Lambda_B$ and hence the paths can be shortened considering the straight line between A and B. ■

D. Optimality conditions for paths between points on C_S

In this subsection, we provide the optimality conditions for paths that cross circumference C_S at least twice before reaching P. Let first consider paths between A and B on C_S, with $\rho_A = \rho_B = \rho_S$ and $|\psi_A - \psi_B| = \Delta\psi$ consisting in pairs of spirals or straight lines that completely evolve in Z_2. We denote such paths with $\mathcal{E}(\Delta\psi) = E_A^{R-} * E_B^{L+}$ where $E \in \{T, S\}$. Notice that paths of type $I_A^{R-} * I_B^{L+}$ are not considered since they violate the H–FOV constraints in Z_2.

Lemma 1: Consider $A = (\rho_S, \Delta\psi)$ and $B = (\rho_S, 0)$ on C_S. The path $\mathcal{E}^{(\infty)}(\Delta\psi)$, consisting of an infinite number of subpaths of type $\mathcal{E}$ with $E \in \{T, S\}$ from A to B, has finite length $L_{\mathcal{E}^{(\infty)}}(\Delta\psi) = L^{(\infty)} = \frac{\rho_S}{\sin\phi}\Delta\psi$.

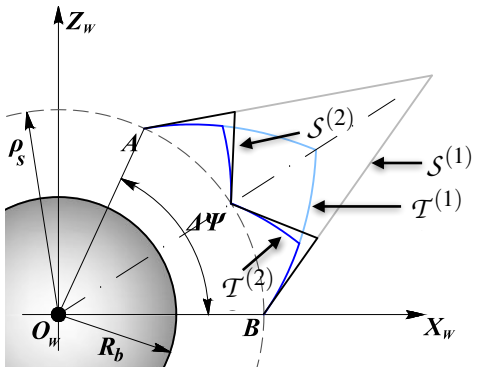

Fig. 6: Paths of type $\mathcal{E}(\Delta\psi) = E_A^{R-} * E_B^{L+}$ with $E \in \{T, S\}$ (i.e. $\mathcal{S}^{(1)}$ and $\mathcal{T}^{(1)}$) and 2 subpaths $\mathcal{E}(\Delta\psi/2)$ forming paths $\mathcal{S}^{(2)}$ and $\mathcal{T}^{(2)}$ respectively. The procedure can be iterated and the path of infinite subpath of type $\mathcal{E}$ has finite length $L_{\mathcal{E}}(\Delta\psi) = \frac{\rho_S}{\sin\phi}\Delta\psi$ (cf. Lemma 1).

Proof: Given two points $A = (\rho_S, \Delta\psi)$ and $B = (\rho_S, 0)$ on C_S let $\mathcal{E}^{(n)}(\Delta\psi)$ be a path from A to B consisting of 2^n subpaths of type $\mathcal{E}(\Delta\psi/2^n)$ of equal length with switching points on C_S. Referring to Fig. 6, notice that for any n, $\mathcal{T}^{(n)}(\Delta\psi)$ and $\mathcal{S}^{(n)}(\Delta\psi)$ are tangent in both A and B. Moreover,

$$L_{\mathcal{T}^{(n)}}(\Delta\psi) \leq L_{\mathcal{S}^{(n)}}(\Delta\psi) \tag{7}$$

for any $n \geq 1$, $\rho_S > R_b$ and $\Delta\psi < 2\phi$. Notice that, inequality (7) holds also for a single pair of extremals and a generic amplitude.

The length of $\mathcal{S}^{(n)}(\Delta\psi)$ decreases for increasing n and converges to $L^{(\infty)} = \frac{\rho_S}{\sin\phi}\Delta\psi$. Indeed, after simple geometrical computations we obtain

$$L_{\mathcal{S}^{(n)}}(\Delta\psi) = 2^n \rho_S \frac{\sin\left(\frac{\Delta\psi}{2^n}\right)}{\sin\left(\phi - \frac{\Delta\psi}{2^n}\right)}.$$

To extend this result to arbitrary amplitude of switches, let us consider inequalities in (7) for $n = 1$ and $\Delta\psi = \delta_i$. We have that $L_{\mathcal{S}}(\delta_i) = 2\rho_S \frac{\sin\frac{\delta_i}{2}}{\sin\left(\phi - \frac{\delta_i}{2}\right)}$ for any $\rho_S > R_b$ and $\delta_i \leq 2\phi$. Based on Taylor expansion it is possible to show that the path consisting in a single pair of straight lines is longer than the path of infinite pairs of same amplitude δ_i, i.e.

$$L_{\mathcal{S}}(\delta_i) = 2\rho_S \frac{\sin\frac{\delta_i}{2}}{\sin\left(\phi - \frac{\delta_i}{2}\right)} \geq \frac{\rho_S}{\sin\phi}\delta_i.$$

Hence, by choosing δ_i such that $\sum_i \delta_i = \Delta\psi$, we obtain that the infimum length of paths consisting in concatenations of pairs of straight lines is $L_{\mathcal{S}^{(\infty)}}(\Delta\psi) = L^{(\infty)}$. Similarly, notice that it also holds

$$L_{\mathcal{T}}(\delta_i) = 2\rho_S \frac{e^{\frac{\delta_i}{2}\cot\phi} - 1}{\cos\phi} \geq \frac{\rho_S}{\sin\phi}\delta_i.$$

As a direct consequence of (7), also the length of $\mathcal{T}^{(n)}(\Delta\psi)$ converges to $L^{(\infty)}$ and hence the infimum length path $\mathcal{T}^{(\infty)}$ consisting in pairs of spiral arcs has finite length $L^{(\infty)} = \frac{\rho_S}{\sin\phi}\Delta\psi$. ■

Notice that the finite length obtained in Lemma 1 does not depend on the typology of path $\mathcal{E}$.

To complete the analysis, it is now necessary to compare the length of the path $\mathcal{T}(\Delta\psi) = T_A^{R-} * T_B^{L+}$, that completely evolves outside C_S, with the length of the path $I(\Delta\psi) = I_A^{L+} * I_B^{R-}$, that completely evolves inside C_S. From [5], if the path $I(\Delta\psi)$ crosses the circumference C_2 it can be shortened by $I_Z(\Delta\psi) = I_A^{L+} * Z * I_B^{R-}$ where Z is an infinite sequence of pairs of involutes of type $I^{R-} * I^{L+}$ on circumference C_2 of length $2R_b\Delta\psi$.

Recalling that $\Psi(\beta) = \tan\beta - \beta$, $I(\Delta\psi)$ is defined for $\Delta\psi \in [0, 2\Psi(\phi)]$, otherwise the switching point between the involutes does not exist. Let $\Delta\psi(\alpha) = 2(\Psi(\phi) - \Psi(\phi - \alpha))$ with $\alpha \in [0, \phi]$ and $\ell_0(\beta) = \frac{R_b}{2\cos^2\beta}$. With an abuse of notation, the lengths of the curves can be expressed as a function of α, as follows:

$$L_I(\alpha) = 2(\ell_0(\phi) - \ell_0(\phi - \alpha)) \text{ if } \alpha \leq \phi - \frac{\pi}{4} \tag{8}$$

$$L_{I_Z}(\alpha) = 2\left(\ell_0(\phi) - \ell_0\left(\frac{\pi}{4}\right)\right) + \\ + 2R_b\left(\Delta\psi(\alpha) - \Delta\psi\left(\frac{\pi}{4}\right)\right) \text{ if } \alpha > \phi - \frac{\pi}{4} \tag{9}$$

$$L_{\mathcal{T}}(\alpha) = \frac{2R_b}{\cos^2\phi}\left(e^{\Delta\psi(\alpha)\cot\phi/2} - 1\right). \tag{10}$$

Remark 5: Based on results reported in [16] Section 2, we have that for any $\alpha \in [0, \phi]$

$$\begin{cases} L_{\mathcal{T}}(\alpha) < L_I(\alpha) & \text{if } \phi \leq \varphi \text{ i.e. } \rho_S \leq \rho_\varphi \\ L_{\mathcal{T}}(\alpha) < L_I(\alpha) & \text{if } \alpha > \bar{\alpha}, \phi \in (\varphi, \pi/4] \text{ i.e. } \rho_\varphi < \rho_S \leq \rho_2 \\ L_I(\alpha) < L_{\mathcal{T}}(\alpha) & \text{if } \alpha \leq \bar{\alpha}, \phi \in (\varphi, \pi/4] \text{ i.e. } \rho_\varphi < \rho_S \leq \rho_2 \\ L_{\mathcal{R}}(\alpha) < L_{\mathcal{T}}(\alpha) & \text{if } \pi/4 < \phi < \pi/2 \text{ i.e. } \rho_2 < \rho_S \end{cases}$$

where $\varphi = \arccos\sqrt{\frac{2}{3}}$, $\rho_\varphi = \sqrt{\frac{3}{2}}R_b \leq \rho_2$, and $\mathcal{R} = I$ for $\alpha \leq \phi - \frac{\pi}{4}$ while $\mathcal{R} = I_Z$ for $\alpha > \phi - \frac{\pi}{4}$. The value of $\bar{\alpha}$ depends on ϕ, refer to [16] Section 2.

Proposition 4: If $\rho_S \leq \rho_2$ the shortest path between two points $A = (\rho_S, \Delta\psi)$ and $B = (\rho_S, 0)$ on C_S does not exist. The path of infimum length consists of infinite switches on C_S and has finite length $L^{(\infty)}$.

Proof: The condition $\rho_S \leq \rho_2$ is equivalent to $\phi \leq \frac{\pi}{4}$. From Remark 5, for such values of ϕ we have that the path $I(\Delta\psi)$ is larger than $\mathcal{T}(\Delta\psi)$ for any $\Delta\psi$ if $\phi \in [0, \varphi]$. From Lemma 1 the path of infimum length consisting in pairs of spiral arcs does not exist and hence the thesis.

Otherwise, from Remark 5, if $\phi \in [\varphi, \pi/4]$, the path $I(\Delta\psi)$ is shorter or equal to $\mathcal{T}(\Delta\psi)$ for $\Delta\psi(\alpha) \leq \Delta\psi(\bar{\alpha})$ while is longer for $\Delta\psi(\alpha) > \Delta\psi(\bar{\alpha})$. For $\Delta\psi(\alpha) \leq \Delta\psi(\bar{\alpha})$, path $I(\Delta\psi)$ can be shortened by a sequence of infinite pairs of involutes of type $I^{L+} * I^{R-}$ with switches on C_S, see results in [5], and hence the thesis.

In case of $\Delta\psi(\alpha) > \Delta\psi(\bar{\alpha})$, path $\mathcal{T}(\Delta\psi)$ is longer than $\mathcal{T}^{(n)}(\Delta\psi)$ for $n > 1$ as shown in Lemma 1. However, there

exists n big enough such that the switches on C_S span an angle smaller than $\Delta\psi(\bar{\alpha})$ and hence $\mathcal{T}^{(n)}(\Delta\psi)$ is shortened by a sequence of infinite pairs of involutes of type $I^{L+} * I^{R-}$ with switches on C_S. ■

From the proof of the previous Proposition $\bar{\alpha}$ does not play an important role since for $\phi \in [\varphi, \pi/4]$ the path of infimum length between $A = (\rho_S, \Delta\psi)$ and $B = (\rho_S, 0)$ corresponds to a sequence of infinite pairs of involutes on C_S of type $I^{L+} * I^{R-}$ for any value of $\Delta\psi$.

The paths $Z^I := \mathcal{I}^{(\infty)}(\Delta\psi)$ and $Z^T := \mathcal{T}^{(\infty)}(\Delta\psi)$ consisting of an infinite number of pairs of involutes and spirals, respectively, with switches on C_S play a similar role of Z in [5] that consists of infinite number of pairs of involutes with switches on C_2.

Proposition 5: If $\rho_S > \rho_2$ the shortest path between two points $A = (\rho_S, \Delta\psi)$ and $B = (\rho_S, 0)$ on C_S is the path $\mathcal{I}(\Delta\psi)$ or does not exist. In the latter, the path of infimum length has finite length given by (9) and it has a subpath which consists of infinite switches on the circumference C_2 of radius ρ_2.

Proof: The condition $\rho_S > \rho_2$ is equivalent to $\phi > \frac{\pi}{4}$. From Remark 5, for such values of ϕ we have that the path $\mathcal{I}(\Delta\psi)$ is smaller than $\mathcal{T}(\Delta\psi)$ for any $\Delta\psi$ if $\phi \in [\pi/4, \pi/2)$. Hence, from the results in [5] for $\Delta\psi \leq \Psi(\phi) - \Psi(\pi/4)$ the optimal path is $\mathcal{I}(\Delta\psi)$. Otherwise, the optimal path does not exist and the path of infimum length is of type $I^{L+} * Z * I^{R-}$ where Z consists of infinite subpath of type $I^{R-} * I^{L+}$ with switches on C_2. Hence, the thesis. ■

E. ε–optimal paths

Even if the lengths of Z, Z^I and Z^T are finite, from a practical point of view, these are impracticable paths. However, depending on the accuracy of motors that move the wheels of the robot, this type of path can be approximated by a finite sequence of involutes or spirals with an error as smaller as more accurate are the motors. A possible approach is to determine an ε–optimal path with a finite number of switches whose length is no longer than any other shorter path more than an arbitrarily small $\varepsilon > 0$. In [5], Remark 6 provides the sufficient number of concatenations of arcs of type $I^{R-} * I^{L+}$ on C_2 obtaining an ε–optimal path Z_ε of Z. In case of $\rho_S \leq \rho_2$, a similar approach can be used for Z^T (if $\phi > \varphi$) and Z^I (if $\phi \leq \varphi$) to obtain ε–optimal paths Z^T_ε and Z^I_ε, respectively.

Remark 6: Consider the case $\phi \leq \varphi$, from Lemma 1 and Remark 5, given $\Delta\psi$, the paths consisting of n subpaths of type $\mathcal{T}(\Delta\psi/n)$ have length $L = 2n\frac{\rho_S}{\cos\phi}\left(e^{\frac{\Delta\psi}{2n\tan\phi}} - 1\right)$, see (10). By truncating the Taylor's series of the exponential function to the second order, we obtain $L - L^{(\infty)} < \frac{\rho_S}{\sin\phi}\frac{\Delta\psi^2}{4\tan\phi}\frac{1}{n}$. Hence, for $n > \frac{\rho_S}{\sin\phi}\frac{\Delta\psi^2}{4\tan\phi}\frac{1}{\varepsilon}$ we have $L - L^{(\infty)} < \varepsilon$. For $\phi \leq \varphi$, from Remark 5, $L_{\mathcal{T}}(\Delta\psi/n) > L_{\mathcal{I}}(\Delta\psi/n)$ hence the same lower bound on n obtained above ensures that the length of the path consisting in n subpaths $\mathcal{I}(\Delta\psi/n)$ is within an ε bound of $L^{(\infty)}$.

F. ε–optimal graphs

The graphs representing possible connections of extremals for the HV–FOV problem are reported in Fig. 7, depending on the value of ϕ which determines the value of ρ_S w.r.t. ρ_φ and ρ_2 which in turn depends only on R_b.

Remark 7: Regarding only the H–FOV case, an additional result w.r.t. [4] is reported in [16] Section 1, further reducing the combination of extremals. This result, shows that any path containing combinations of type $S^+ * T^{R-}$ and $T^{L+} * S^-$ is not optimal. As a consequence, the subgraph of the ε-optimal graphs in Fig. 7 related to the H–FOV constraint has a reduced number of links w.r.t. the one reported in [4].

Conversely to the H–FOV optimal synthesis developed in [4], the result summarized in previous Remark 7 will be necessary and important in the following analysis of this paper. Indeed, differently from [4], without excluding $S^+ * T^{R-}$ and $T^{L+} * S^-$, here it is not possible to exclude loops in the graphs reported in Fig. 7 and hence the consequent no existence of optimal paths.

Notice that, for $\rho_S \leq \rho_\varphi$ (cf. Fig. 7(a)) the switches between T^{R-} and T^{L+} can be infinite and occur on C_S. Moreover, when $\rho_\varphi < \rho_S \leq \rho_2$ (cf. Fig. 7(b)) switches are between I^{R-} and I^{L+}, can be infinite and still occur on C_S. Finally, for any $\rho_S > \rho_2$ (cf. Fig. 7(c)) the infinite switches between I^{R-} and I^{L+} occur on C_2.

Moreover, from Proposition 4 and Proposition 7 in [5], the extremals Z^T_ε, Z^I_ε or Z_ε may occur only once in an infimum length path. Indeed, when $\rho_S \leq \rho_2$ from Proposition 4 the path of infimum length between two points on C_S is the extremal Z^T_ε or Z^I_ε. Finally, for $\rho_2 < \rho_S$ from the V–FOV–synthesis the path of infimum length between two points on C_2 is the extremal Z_ε.

To conclude, a path of infimimum length corresponds to a finite number of possible concatenations of extremals as reported in Fig. 7. Hence, the paths of infimum length are of type $S^+T^{L+}I^{L+} * \mathcal{E} * I^{R-}T^{R-}S^-$ with $\mathcal{E} \in \{Z^T_\varepsilon, Z^I_\varepsilon, Z_\varepsilon\}$ where the switches between arcs T and I are on C_S.

IV. Regions inherited from the H–FOV and the V–FOV Synthesis

Given initial and final points $Q, P \in Z_1$ (Z_2) respectively, if the infimum path length from Q to P for the V–FOV (H–FOV) synthesis does not intersect C_S then it is also an infimum length path for the HV–FOV synthesis. If point $Q \in Z_1$ and point $P \in Z_2$ (or vice–versa), the path is of infimum length also for the HV–FOV synthesis if it intersects C_S inside Ω_P or Λ_P. Indeed, inside Ω_P or Λ_P, C_S can be crossed with a straight line and from Proposition 3 the optimal concatenation of two arcs S is smooth on C_S. As a consequence, there are regions of the HV–FOV synthesis that are completely or partially inherited from the two previously obtained synthesis. The shape of such regions depends on the value of ϕ and hence on where C_S intersects the H–FOV and the V–FOV synthesis.

In Fig. 8, an example of the inherited regions from the H–FOV and the V–FOV is reported. In this example, we have $\rho_2 < \rho_S < \rho_5 < \rho_P$ with $\phi = \pi/4$ and point P is far enough from O_W. This value of ϕ is the FOV aperture of the most standard cameras and has been chosen as a high probable practical scenario that will be deeply analyzed throughout the paper. However, other two cases with different horizontal apertures

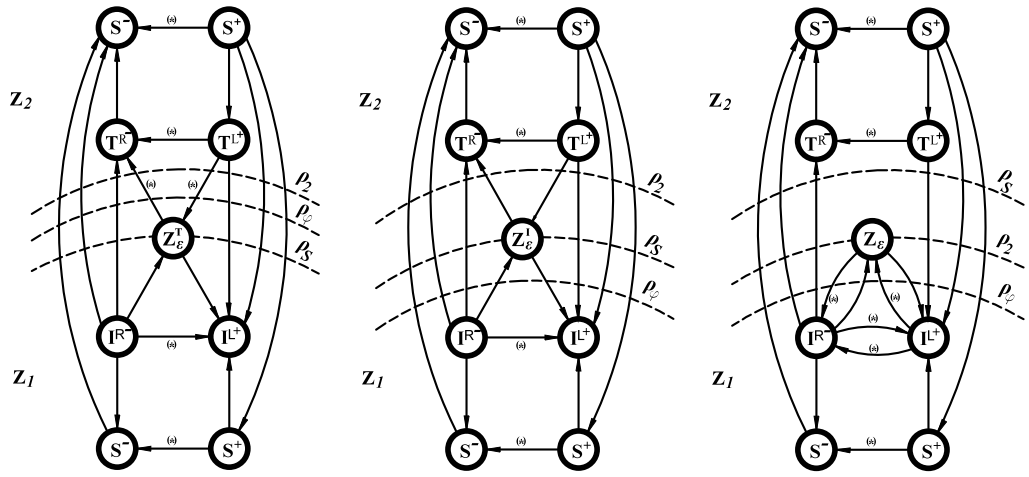

(a) Case of $\rho_S \leq \rho_\varphi$. (b) Case of $\rho_\varphi < \rho_S \leq \rho_2$. (c) Case of $\rho_2 < \rho_S$.

Fig. 7: Feasible extremals and sequences of extremals from points in $Z_1 \cup Z_2$.

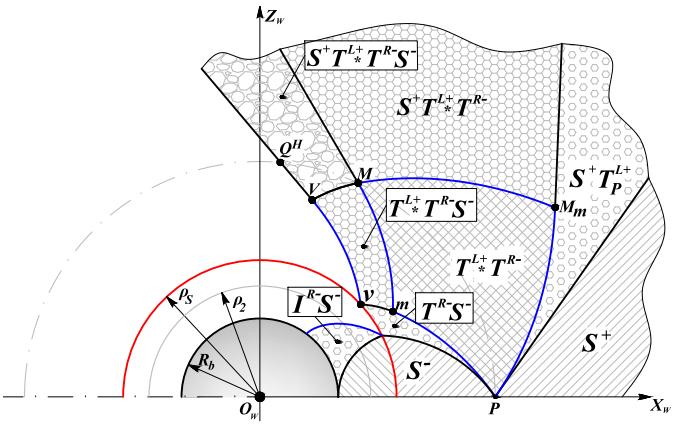

Fig. 8: Example of inherited regions from the H–FOV and the V–FOV synthesis with ϕ such that $\rho_2 < \rho_S < \rho_5 < \rho_P$ and $\rho_P > \frac{R_b}{\cos\phi \sin^2\phi}$. For any region, the type of the inherited infimum length path from that region to P is reported.

ϕ, bigger ($\approx \pi/3$) and smaller ($\approx \pi/5$) w.r.t. the case in Fig. 8 are reported in [16] Section 3 with the same values for P and $\hat{\phi}$.

Referring to Fig. 8, from the H–FOV synthesis, $m = (\rho_m, \psi_m) = (\rho_P \sin^2\phi, -2\tan\phi \log\sin\phi)$ and $\rho_m > \rho_S$ if and only if $\rho_P > \frac{R_b}{\cos\phi \sin^2\phi}$. Hence, in this case, the region of the H–FOV synthesis characterized by the optimal path of type $T^{L+} * T^{R-}$ (called Region II in [4]) is completely inherited and characterizes the optimal path from that region to P also for the HV–FOV synthesis. This is true also for the regions characterized by path $S^+T^{L+} * T^{R-}$, S^+T^{L+} and S^+.

From point m, the circular arc C_m^R crosses circumference C_S in $v = (\rho_S, \psi_m + \phi - \arcsin\left(\frac{2R_b}{\rho_P \sin(2\phi)}\right)$ (see Fig. 8). Let $Q^H \in CP$ be such that the optimal path from Q^H toward P touches, without crossing, the circumference C_S in v. Hence, it completely evolves in Z_2 and it is the last path inherited from the H–FOV synthesis. Indeed, from point $Q \in CP$ with $\psi_Q > \psi_{Q^H}$, paths of the H–FOV synthesis necessarily cross circumference C_S, leading to a not optimal path for the HV–FOV case. The path from Q^H is a palindrome path of type $S^+T^{L+} * T^{R-}S^-$ where the rotation on the spot $*$ is performed exactly in v. As a consequence, $Q^H = (\rho_P, 2\psi_v)$. The Region IV in [4], characterized by the palindrome path $S^+T^{L+} * T^{R-}S^-$, is hence partially inherited in the HV–FOV synthesis and its shape depends on the position of point m w.r.t. C_S. The same also holds for the regions characterized by paths of type $S^+T^{L+} * T^{R-}$ and $T^{R-}S^-$.

Still referring to the example reported in Fig. 8 where $\rho_S < \rho_5$, it is worth noting that the only region (partially) inherited from the V–FOV synthesis is in Z_1 and is characterized by the optimal path of type $I^{R-}S^-$. To conclude, the backward straight line regions inherited from the H–FOV and V–FOV synthesis is given by Proposition 2.

The generalization of this analysis to other cases is straightforward. Indeed, if $\rho_P = \frac{R_b}{\cos\phi \sin^2\phi}$, point $m \in C_S$, $Q^H \equiv M = (\rho_P, 2\psi_m)$ and the optimal path from Q^H to P is now of type $T^{L+} * T^{R-}$. This path is optimal also if $\rho_P < \frac{R_b}{\cos\phi \sin^2\phi}$. However, in this case, point m is inside C_S, $Q^H = (\rho_P, 2\tan\phi \log\left(\frac{\rho_P \cos\phi}{R_b}\right))$ and the Region II is only partially inherited as well as the region characterized by the path $S^+T^{L+} * T^{R-}$. On the other hand, if $\phi \geq \arccos\sqrt{5}$, i.e. $\rho_S \geq \rho_5$, and $\rho_P > \rho_5$, the region in Z_1 characterized by the optimal path $I^{R-}S^-$ is now completely inherited from the V–FOV synthesis. Similar reasoning can be done in case of $\rho_P < \rho_S$.

V. Synthesis for $\rho_S \in [\rho_2, \rho_5]$ and $\rho_P > \rho_S$

Given the results above, for initial and final points Q and P respectively, the HV–FOV synthesis depends on their position with respect to C_S and the value of ρ_S. For the sake of brevity, we provide a detailed description of the synthesis for $\rho_S \in [\rho_2, \rho_5]$ and $\rho_P > \rho_S$, i.e. the horizontal FOV is such that $\phi \geq \pi/4$. The synthesis for the other cases can be obtained with a similar approach as described in [16] Section 3.

We first introduce and recall the notation that will be used in the synthesis construction. Let C_5 and C_N be the circumferences centered in the origin with radii $\rho_5 = \sqrt{5}R_b$ and $\rho_N = 2R_b/\sin\phi$. It is worth noticing that $\rho_S < \rho_5 < \rho_N$ for $\tan\phi < 2$ and $\rho_N < \rho_5 < \rho_S$ for $\tan\phi > 2$ while $\rho_S = \rho_5 = \rho_N$ for $\tan\phi = 2$. Similarly to the procedure followed in [4] and [5], in order to obtain the overall synthesis, we start analyzing the infimum length paths from points Q on the circumference CP of radius ρ_P to $P = (\rho_P, 0)$. The goal is to first obtain the synthesis of the circumference CP and then to extend it to the whole plane of motion. The graph representing the sequences of extremals for the case under consideration is the one reported in Fig. 7(c) and hence from points on CP the infimum length paths to P are palindrome paths of type $S^+T^{L+}I^{L+} * Z * I^{R-}T^{R-}S^-$ where Z lays on C_2 while switching points between spiral and involute arcs lay on C_S where $\rho_S \geq \rho_2$. For the sake of simplicity we start analyzing the paths from the point $Q_0 = (\rho_P, \pi) \in CP$ (see Fig. 9). The case $Q = (\rho_P, \psi_Q) \in CP$ with $0 \leq \psi_Q \leq \pi$ will also follow from this analysis.

Proposition 6: Consider $P = (\rho_P, 0)$ and $Q_0 = (\rho_P, \pi) \in CP$ with $\rho_P > \rho_N$ and $\rho_S \in [\rho_2, \rho_5]$, the path of infimum length from Q_0 to P is a palindrome path of type $S^+T^{L+}I^{L+} * Z * I^{R-}T^{R-}S^-$ with intersection points $P_N \in C_N \cap \partial\Omega_P$ between T^{R-} and S^-, $P_S \in C_S$ between I^{R-} and T^{R-}, P_2 on C_2 between Z and I^{R-},

Proof: Based on simple computations, the arc Z has no zero length if $\rho_P < \hat{\rho} = \frac{R_b}{\cos\phi} e^{\frac{1}{\tan\phi}\left(\frac{3}{4}\pi - 1 + \tan\phi - \phi\right)}$. Hence, for such ρ_P, from the palindromy property (see Definition 2), it is sufficient to study the sub–path from $Q_1 = (\rho_2, \pi/2) \in C_2$ to P of type $Z * I^{R-}T^{R-}S^-$ (see Fig. 9). Let β be the heading angle in P used to parametrize the path length (see Fig. 9) and the switching point $V = (\rho_V, \psi_V)$, between T^{R-} and S^-, be on ∂C_P with $\rho_S \leq \rho_V \leq \rho_P$. By the sine rule we have $\rho_V = \rho_P \frac{\sin\beta}{\sin\phi}$ and $\psi_V = \phi - \beta$. The logarithmic spiral through V is $\rho = \rho_V\, \mathrm{e}^{(\psi_V - \psi)t}$, $t = \frac{1}{\tan\phi}$, and it intersects C_S in $W = (\rho_S, \psi_S)$ where

$$\rho_S = \frac{R_b}{\cos\phi} = \rho_P \frac{\sin\beta}{\sin\phi}\, \mathrm{e}^{(\psi_V - \psi_S)t}$$

and hence $\psi_S = \psi_V + \tan\phi \ln\left(\frac{\rho_P \sin\beta}{R_b \tan\phi}\right)$. The straight line arc S between P and V has length

$$L_S = \rho_P \frac{\sin(\phi - \beta)}{\sin\phi}$$

while the length of the logarithmic spiral arc between V and W is

$$L_T = \frac{\rho_V - \rho_S}{\cos\phi} = \frac{2(\rho_P \sin\beta - R_b \tan\phi)}{\sin 2\phi}$$

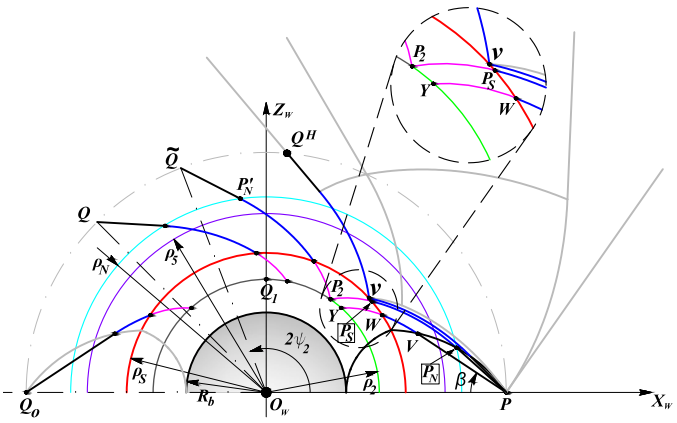

Fig. 9: Analysis of palindrome paths of type $S^+T^{L+}I^{L+} * Z * I^{R-}T^{R-}S^-$ from point $Q_0 = (\rho_P, \pi)$ to $P = (\rho_P, 0)$ and generalization to any point on CP between Q_0 and Q^H.

Starting from W the path evolves in Z_1 by an involute arc that ends in Y on C_2 (see Fig. 9) and its length is

$$L_I = \frac{R_b}{2}\left(\frac{1}{\cos^2\phi} - 2\right).$$

The angle ψ_Y is

$$\psi_Y = \phi - \beta + \tan\phi \ln\left(\frac{\rho_P \sin\beta}{R_b \tan\phi}\right) + \tan\phi - \phi - 1 + \frac{\pi}{4},$$

and hence the length of the arc Z from Q_1 to Y is

$$L_Z = 2R_b\left(\frac{\pi}{2} - \psi_Y\right).$$

The total path length becomes $L(\beta) = L_S + L_T + L_I + L_Z$ and its minimum for $\rho_S \leq \rho_V \leq \rho_P$ or equivalently $\arcsin\left(\frac{R_b}{\rho_P}\tan\phi\right) \leq \beta \leq \phi$ is such that

$$\frac{\partial L}{\partial \beta} = -\left(\rho_P - 2\frac{R_b}{\sin\beta}\right)\frac{\sin(\beta - \phi)}{\cos\phi} = 0.$$

Let C_N be the circumference centered in O_w of radius $\rho_N = \frac{2R_b}{\sin\phi}$. For $\rho_P > \rho_N$ the function L has a maximum in ϕ and a minimum in $\beta^* = \arcsin\left(\frac{2R_b}{\rho_P}\right)$ if $\beta^* \geq \arcsin\left(\frac{R_b}{\rho_P}\tan\phi\right)$, i.e. if $\rho_S \leq \rho_5$ (or equivalently $\phi \leq \arctan 2$). Substituting the optimal value β^* in ρ_V we obtain that the switching between T^{R-} and S^- occurs in $V = P_N = (\rho_N, \phi - \beta^*) \in C_N$, whose radius does not depend on ρ_P, if $\rho_S \leq \rho_5$.

Referring to Fig. 9, the switch between I^{R-} and T^{R-} occurs in $W = P_S = (\rho_S, \psi_S) \in C_S$ (where $\psi_S = \psi_N - \tan\phi \log\left(\frac{\tan\phi}{2}\right)$) while the one between Z and I^{R-} in $Y = P_2 = (\rho_2, \psi_S + \tan\phi - \phi - \frac{3}{4}\pi) \in C_2$. ■

Based on Proposition 6 we can now compute the synthesis of the semicircle CS.

Proposition 7: Given $Q = (\rho_P, \psi_Q) \in CP$, the path of infimum length from Q to P is

1) $S^+T^{L+} * T^{R-}S^-$ or $T^{L+} * T^{R-}$ for $0 \leq \psi_Q \leq \psi_{Q^H}$ as described in the H–FOV synthesis in [4], i.e. for any point on CP between Q^H and P,
2) $S^+T^{L+}I^{L+} * I^{R-}T^{R-}S^-$, for $\psi_{Q^H} < \psi_Q \leq \psi_{\tilde{Q}}$, i.e. for any point on CP between $\tilde{Q}$ and Q^H,
3) $S^+T^{L+}I^{L+} * Z * I^{R-}T^{R-}S^-$ with switching point $P_2 \in C_2$ between Z and I^{R-} and $P_S \in C_S$ between I^{R-} and T^{R-} and $P_N \in C_N$ between T^{R-} and S^-, for $\psi_{\tilde{Q}} < \psi_Q \leq \pi$, i.e. for any point on CP between $Q_0 = (\rho_P, \pi)$ and $\tilde{Q}$.

Proof:

1) See results reported in Section IV.

2) Let us now consider $Q = (\rho_P, \psi_Q)$ with $\psi_Q > \psi_{Q^H}$. The optimal path for Q to P, obtained in the H–FOV synthesis, intersects C_S in at least two points (since $\rho_S < \rho_P$) and hence the path violates the V–FOV constraint between those points. Based on the graph in Fig. 7(c), the path of infimum length from Q to P is of type $S^+T^{L+}I^{L+} * Z * I^{R-}T^{R-}S^-$ where arcs may have zero length. For $\psi_{Q^H} \leq \psi_Q < \psi_{\tilde{Q}}$ there exist values of β_Q such that the path of type $S^+T^{L+}I^{L+} * Z * I^{R-}T^{R-}S^-$ degenerates in $S^+T^{L+}I^{L+} * I^{R-}T^{R-}S^-$. For such values a comparison between such paths lengths must be carried out. For space limitations an exhaustive analysis of the comparison can not be reproduced. In Fig. 10(a) the length of paths of types $S^+T^{L+}I^{L+} * Z * I^{R-}T^{R-}S^-$ (in blue) and $S^+T^{L+}I^{L+} * I^{R-}T^{R-}S^-$ (in red) is plotted for different values of the parameter β that represents the heading angle in P and in Q. Three curves representing different values of ψ_Q are reported. The lowest curve represents the length of the paths for $\psi_{Q^H} \leq \psi_Q < \psi_{\tilde{Q}}$ for which the minimum is reached by a path of type $S^+T^{L+}I^{L+} * I^{R-}T^{R-}S^-$. The curve in between corresponds to the case $\psi_Q = \psi_{\tilde{Q}}$ in which the infimum path $S^+T^{L+}I^{L+} * Z * I^{R-}T^{R-}S^-$ degenerates to $S^+T^{L+}I^{L+} * I^{R-}T^{R-}S^-$, hence $\beta_{\tilde{Q}} = \beta^*$ and the path $\gamma_{\tilde{Q}}$ is optimal. In Fig. 10(b) the case $\psi_{Q^H} < \psi_Q \leq \psi_{\tilde{Q}}$ is considered to highlight how, in this case, the value of the parameter associated to the optimal path changes with ψ_Q. In particular it increases while the value of ψ_Q decreases to ψ_{Q^H}. Hence the infimum length paths from $Q = (\rho_P, \psi_Q)$ with $\psi_{Q^H} < \psi_Q \leq \psi_{\tilde{Q}}$ to P are of type $S^+T^{L+}I^{L+} * I^{R-}T^{R-}S^-$.

3) Finally, consider a point $Q = (\rho_P, \psi_Q) \in CP$ with $\psi_{\tilde{Q}} < \psi_Q \leq \pi$ and the paths of type $S^+T^{L+}I^{L+} * Z * I^{R-}T^{R-}S^-$. Notice that, since $\gamma_{\tilde{Q}}$ is optimal from $\tilde{Q}$ to P, for $\psi_Q > \psi_{\tilde{Q}}$ there exists no degenerate optimal path of type $S^+T^{L+}I^{L+} * I^{R-}T^{R-}S^-$ from Q to P, i.e. a non zero length arc Z is part of the infimum length path. For $\psi_Q \in [\psi_{\tilde{Q}}, \pi]$ an analysis equivalent to the one reported in the proof of Proposition 6 can be done obtaining that the infimum length path has P_2 as the switching point between Z and I^{R-}, i.e. the subpath $I^{R-}T^{R-}S^-$ does not depend on ψ_Q while the only dependency is in the length of arc Z. Indeed, in Fig. 10(a), the highest curve represents the length of the paths $S^+T^{L+}I^{L+} * Z * I^{R-}T^{R-}S^-$ and $S^+T^{L+}I^{L+} * I^{R-}T^{R-}S^-$ for $\pi \leq \psi_Q < \psi_{\tilde{Q}}$ for which the minimum is reached for a constant value of $\beta^* = \arcsin\left(\frac{2R_b}{\rho_P}\right)$ and corresponds to a path of type $S^+T^{L+}I^{L+} * Z * I^{R-}T^{R-}S^-$. It is hence possible to show that the statement of the Proposition 6 holds for any $Q = (\rho_P, \psi_Q) \in CP$ with $\psi_Q \in [\psi_{\tilde{Q}}, \pi]$. ■

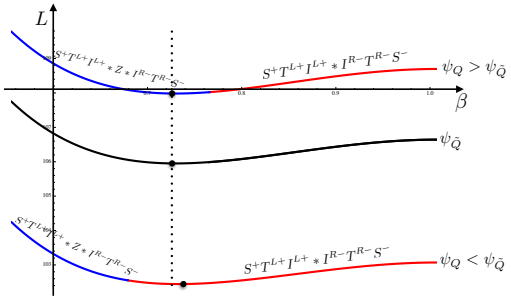

(a) Length of paths of type $S^+T^{L+}I^{L+} * Z * I^{R-}T^{R-}S^-$ w.r.t. values of β and different values of ψ_Q.

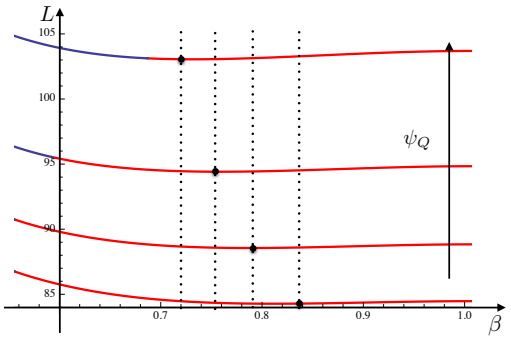

(b) Length of paths of type $S^+T^{L+}I^{L+} * Z * I^{R-}T^{R-}S^-$ w.r.t. values of β and different values of $\psi_Q < \psi_{\tilde{Q}}$. Notice that the value of β, corresponding to the minimum of the length, increases while the value of ψ_Q decreases to ψ_{Q^H}.

Fig. 10: Lengths of paths of type $S^+T^{L+}I^{L+} * Z * I^{R-}T^{R-}S^-$ and of type $S^+T^{L+}I^{L+} * I^{R-}T^{R-}S^-$.

Having the synthesis of CS, the extension of this result in the semi-disk DS can be done by using the following simple idea: for any $Q \in DS$, find a point in $S \in CS$ such that an infimum length path from S to P goes through Q. By Bellmann's Optimality Principle, the subpath from S to P is also an infimum length path. Consider the partition of DS in sixteen regions illustrated in Fig. 11. Regions are generalized polygonals characterized by vertices and whose boundaries belong either to the extremal curves or to the switching loci. Such regions characterize the optimal synthesis as stated in the following theorem that summarizes one of the main contributions of this paper.

Theorem 1: For $\rho_P > \rho_N$ and $\rho_S \in [\rho_2, \rho_5]$, the synthesis of the upper half–plane taking into account the infimum path length Z as an extremal, is described in Fig. 11 and Table II. For each region, the associated path type entirely defines a path of infimum length to the goal.

The notation used in the table is based on the synthesis provided in [4] and [5]. For example, Region VI_C^H is region VI_C of the H–FOV synthesis that is inherited in the HV–FOV synthesis (see Section IV). Notice that Region I consists in

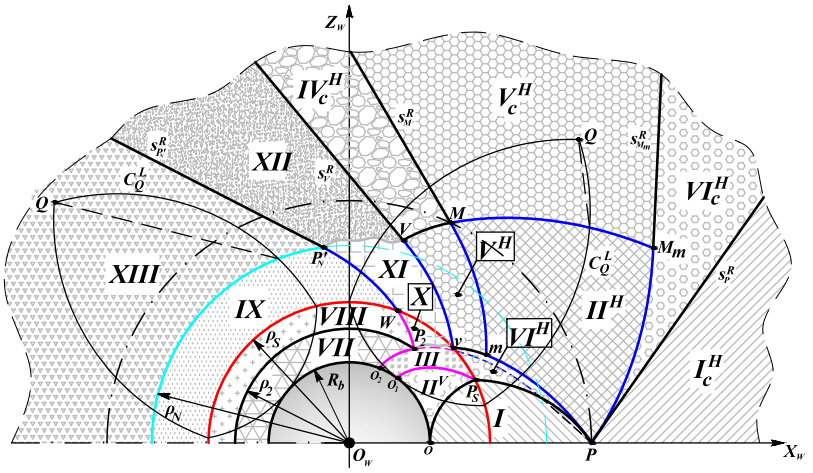

Fig. 11: HV–FOV synthesis in case of $\rho_P > \rho_N$ and ϕ such that $\rho_2 \le \rho_S \le \rho_5$.

Point	Polar coordinates (ρ, ψ)
P	$(\rho_P, 0)$
P_S	$(\rho_S, \phi - \arcsin\left(\frac{R_b}{\rho_P}\tan\phi\right))$
M_m	$(\frac{\rho_P}{\sin\phi}, -2\tan\phi\log\sin\phi)$
m	$(\rho_P\sin^2\phi, -2\tan\phi\log\sin\phi)$
v	$(\rho_S, \phi - \arcsin\left(\frac{2R_b}{\rho_P\sin(2\phi)}\right) + \psi_m)$
O_1	$(R_b, \psi_{P_S} + \phi - \tan\phi)$
P_2	$(\rho_2, \hat{\psi} - \arcsin\left(\frac{2R_b}{\rho_P}\right) + \frac{\pi-4}{4})$
M	$(\rho_P, -4\tan\phi\log\sin\phi)$
O_2	$(R_b, \psi_{P_2} + \arccos\frac{1}{\sqrt{2}} - \tan\arccos\frac{1}{\sqrt{2}})$
W	$(\rho_S, \psi_{P_2} + \tan\phi - \phi + \frac{\pi-4}{4})$
V	Solution of...
P_N'	$(\frac{2R_b}{\sin\phi}, \psi_W + \tan\phi\log\left(\frac{2}{\tan\phi}\right))$

TABLE I: Points of the synthesis in Fig. 11, where $\hat{\psi} = \tan\phi\left(1+\log\left(\frac{2}{\tan\phi}\right)\right)$. Points are sorted by increasing values of ψ if $\phi > \arccos\left(1/(2\sqrt{2}-1)\right)$.

the union of I^H and I^V. The curves γ_{P_S} and γ_V do not have particular geometric characteristics. Their explicit expressions, which are not reported here for the sake of space, can be found based on the computations and considerations done in Propositions 6 and 7.

We are now able to prove Theorem 1.

Proof: (Theorem 1) Referring to Fig. 11, the proof is done considering each region separately. Notice that the proof for inherited regions can be found in [4] and [5], see Section IV.

***Region* I**: From any point in this region it is possible to reach P with a straight path in backward motion without violating the HV–FOV constraints since it is the intersection of straight line regions for the two separated synthesis.

***Region* IX**: From any point Q in this region there exists a point $Q' \in CP$ such that for Proposition 7 the infimum path from Q' to P (of type $S^+T^{L+}I^{L+}*Z*I^{R-}T^{R-}S^-$) passes through Q. Hence, the path of infimum length from Q to P is the subpath of type $T^{L+}I^{L+}*Z*I^{R-}T^{R-}S^-$.

***Region* VIII**: From any point Q in this region there exists a point $Q' \in C_S$ such that, from previous point, the infimum path from Q' to P passes through Q. Hence, the path of infimum length from Q to P is the subpath of type $I^{L+}*Z*I^{R-}T^{R-}S^-$.

***Region* XIII**: From any point $Q \in CP$ in this region the infimum path from Q to P is of type $S^+T^{L+}I^{L+}*Z*I^{R-}T^{R-}S^-$. By varying the length of path S^+ from zero to infinite the path of minimum length from any point of the region to P is constructively obtained.

***Region* X**: From any point Q in this region there exists a point $Q' \in CP$ such that for Proposition 7 the infimum path from Q' to P (of type $S^+T^{L+}I^{L+}*I^{R-}T^{R-}S^-$) passes through Q. Hence, the path of infimum length from Q to P is the subpath of type $I^{L+}*I^{R-}T^{R-}S^-$.

***Region* XI**: From any point Q in this region there exists a point $Q' \in CP$ such that for Proposition 7 the infimum path from Q' to P (of type $S^+T^{L+}I^{L+}*I^{R-}T^{R-}S^-$) passes through Q. Hence, the path of infimum length from Q to P is the subpath of type $T^{L+}I^{L+}*I^{R-}T^{R-}S^-$.

***Region* XII**: Similarly to Region XIII, from any point $Q \in CP$ in this region, the infimum path from Q to P is of type $S^+T^{L+}I^{L+}*I^{R-}T^{R-}S^-$. By varying the length of path S^+ from zero to infinite the path of minimum length from any point of the region to P is constructively obtained.

***Region* VII**: From the V–FOV synthesis from points inside C_2 arcs of type I^{L+} or I^{R+} do not belong to infimum length paths that reach points outside C_2. Hence, from such points the only possible way to reach C_2 is with an arc of type I^{R-}, see the graph in Fig. 7(c). Thus, the infimum path length from points of this region are of type $I^{R-}Z*I^{R-}T^{R-}S^-$.

***Region* III**: From points in this region, that belong to optimal paths from points in Region XII, the optimal path is of type $I^{R-}T^{R-}S^-$. From all other points the same analysis provided in Proposition 6 can be done (starting from points on C_2) obtaining that in the optimal path the length of arc Z is zero and hence the optimal path is of type $I^{R-}T^{R-}S^-$. ■

The complete HV–FOV synthesis with $\phi = \pi/4$ and $\rho_P > \rho_N$ is reported in Fig. 11.

To conclude the analysis for $\rho_P > \rho_S$ and $\rho_S \in [\rho_2, \rho_5]$ the case $\rho_P \le \rho_N$ must be considered.

Lemma 2: Consider $P = (\rho_P, 0)$ and $Q = (\rho_P, \pi) \in CP$ with $\rho_S \le \rho_P \le \rho_N$, the path of infimum length from Q to P is of type $T^{L+}I^{L+}*Z*I^{R-}T^{R-}$ with intersection points $P_S \in C_S$ between I^{R-} and T^{R-} and $P_2 \in C_2$ between Z and I^{R-}.

Proof: For $P = (\rho_P, 0)$ and $Q = (\rho_P, \pi) \in CP$, with $\rho_P \le \rho_N$ and $\rho_S \in [\rho_2, \rho_5]$ the same proof of Proposition 6 can be applied. In this case, the function L has a minimum in $\beta^* = \phi$. Hence arc S^- has zero length and the infimum length path is of type $T^{L+}I^{L+}*Z*I^{R-}T^{R-}$. The switching point between I^{R-} and T^{R-} is $P_S = (\rho_S, \psi_S) \in C_S$ (where $\psi_S = \tan\phi\log\left(\frac{\rho_P\cos\phi}{R_b}\right)$) and the one between Z and I^{R-} is $P_2 = (\rho_2, \psi_S + \tan\phi - \phi - \frac{3}{4}\pi) \in C_2$. ■

To extend this result to the case $Q = (\rho_Q, \pi)$ with $\rho_Q > \rho_P$

we can compute the path of infimum length from Q to P by applying Theorem 1 and switching initial and final points P and Q, i.e. considering P and Q as initial and final points respectively. Hence, by reproducing the same reasoning proposed for $\rho_P > \rho_N$, a similar synthesis is obtained where the roles of points P_S and P_2 of that case are covered by the new points $P_S \in C_S \cap T_P^R$ and $P_2 \in C_2 \cap I_{P_S}^R$ whose coordinates have been computed in the proof of Lemma 2. Moreover, it is also possible to show that for points Q from which the infimum length paths are of type $S^+T^{L+}I^{L+} * Z * I^{R-}T^{R-}$, the locus of switching points between S^+ and T^{L+} is on C_N.

The extension to the general case $Q = (\rho_Q, \psi_Q)$ can be obtained with a similar approach used for previous synthesis, see e.g. Proposition 6.

VI. On the practical use of the HV–FOV synthesis

In the previous sections, the HV–FOV synthesis in case of $\rho_P > \rho_N$ and ϕ such that $\rho_2 \leq \rho_S \leq \rho_5$ has been provided. The goal is now to describe a method to establish where the initial point Q lays w.r.t. the partition given in Fig. 11, and to compute the infimum length path from Q to P.

First let $\rho(\psi)$ be the distance to the origin with respect to the angle ψ along the curves that represent the borders of Regions. The list of borders can be found in the third column of Table II where only included boundaries are reported for each region. All borders in the third column can be characterized by two (limit) values of the angle ψ and by one (limit) value of $\rho(\psi)$. The Region $Q = (\rho_Q, \psi_Q)$ belongs to can be hence determined by verifying two inequalities for ψ_Q and one for ρ_Q. The functions $\rho(\psi)$ are in closed form or are determined as a solution of non linear algebraic equations as described in [4] and in [5] and omitted here for the sake of space. An efficient way to determine the regions of the synthesis in which $Q = (\rho_Q, \psi_Q)$ lays is the following. Consider the 12 points p_i, $i = 1, \ldots, 11$, reported in Table I ordered with increasing value of ψ_{p_i}, i.e. $p_1 = P$ and $p_{12} = P'_N$. Notice that it always holds $\psi_m = \psi_{M_m}$ while the order of points between P and P'_N can change based on the value of ϕ. Determine the points j and $j+1$ such that $\psi_{p_j} \leq \psi_Q \leq \psi_{p_{j+1}}$ with $j = 1, \ldots, 10$. Referring to Fig. 11 the point Q in region XIII verifies $\psi_Q > \psi_{12}$ while the point Q in region V_c^H verifies $\psi_v = \psi_5 \leq \psi_Q \leq \psi_6 = \psi_{O_1}$.

Region	Included Vertices	Included Boundaries	Optimal Path Type
I	O, P_S, P	$\partial\Omega_P$	S^-
I_c^H	P	s_P^R	S^+
II^V	P_S, O, O_1	Lim_P^R, ∂Z_0, $I_{P_S}^R$	$I^{R-}S^-$
II^H	P, M, m, M_m	T_P^R, T_M^L, T_P^L, T_M^R	$T^{L+} * T^{R-}$
III	P_S, v, P_2, O_2, O_1	$I_{P_S}^R$, C_S, γ_v, $I_{P_2}^R$, ∂Z_0	$I^{R-}T^{R-}S^-$
IV_c^H	V, M	s_M^R, s_V^R, C_M^R	$S^+T^{L+} * T^{R-}S^-$
V^H	v, m, M, V	C_m^R, T_M^L, C_M^R, T_V^L	$T^{L+} * T^{R-}S^-$
V_c^H	M, M_m	$s_{M_m}^R$, s_M^R, $T_{M_m}^R$	$S^+T^{L+} * T^{R-}$
VI^H	P, m, v, P_S	T_P^R, C_m^R, C_S, C_P^R	$T^{R-}S^-$
VI_c^H	P, M_m	$s_{M_m}^R$, s_P^R, $T_{M_m}^L$	S^+T^{L+}
VII	P_2, O_2	$I_{P_2}^R$, ∂Z_0, X_W, C_2	$I^{R-}Z * I^{R-}T^{R-}S^-$
VIII	P_2, W	I_W^L, C_S, X_W, C_2	$I^{L+} * Z * I^{R-}T^{R-}S^-$
IX	W, P'_N	$I_{P'_N}^L$, C_N, X_W, C_S	$T^{L+}I^{L+} * Z * I^{R-}T^{R-}S^-$
X	v, W, P_2	C_S, I_W^L, γ_v	$I^{L+} * I^{R-}T^{R-}S^-$
XI	v, V, P'_N, W	T_V^L, γ_V, $T_{P'_N}^L$, C_S	$T^{L+}I^{L+} * I^{R-}T^{R-}S^-$
XII	V, P'_N	γ_V, s_V^R, $s_{P'_N}^R$	$S^+T^{L+}I^{L+} * I^{R-}T^{R-}S^-$
XIII	P'_N	$s_{P'_N}^R$, C_N, X_W	$S^+T^{L+}I^{L+} * Z * I^{R-}T^{R-}S^-$

TABLE II: Detailed description of the HV–FOV synthesis represented in Fig. 11.

Table III reports for each range of ψ_Q the borders for which $\rho(\psi_Q)$ must be compared with ρ_Q. Notice that in the worst case, at most 8 inequalities of the form $\rho(\psi_Q) - \rho_Q \leq 0$ must be evaluated. This procedure is hence very efficient in terms of computational costs once $\rho(\psi_Q)$ is computed for all the borders. For example, referring to Fig. 11, the point Q in region XIII has $\psi_Q \in [\psi_{P'_N}, \pi]$ and ρ_Q is larger than the $\rho(\psi_Q)$ associated to C_N and smaller than the $\rho(\psi_Q)$ associated to $s_{P'_N}^R$. The point Q in region V_c^H verifies $\psi_Q \in [\psi_v, \psi_{O_1}]$ while ρ_Q is larger than the $\rho(\psi_Q)$ associated to $T_{M_m}^R$ and smaller than the $\rho(\psi_Q)$ associated to $s_{M_m}^R$.

Once the vehicle is localized with respect to the synthesis, the infimum path length can be easily computed as follows. Each region of the synthesis is characterized by one type of extremal arc, i.e. the first arc of the infimum length paths from that region to P (see Table II). Moreover, such arcs may coincide with a border or connect two different borders of the regions. For example, while the vehicle crosses Region II^H, it follows an arc of spiral of type T^L that may coincide with borders T_P^L or T_M^L or connect border T_M^R with border T_P^R (see Table II). Arcs associated to regions are reported in Table IV for reader convenience.

In case of regions characterized by arcs of type T^R, T^L, I^R or I^L, the infimum length path is univocally determined since for each point Q in those regions there exists one and only one spiral arc or involute arc (left or right) passing through Q. Given a point $Q = (\rho_Q, \psi_Q)$, explicit equations of spirals T

Value of ψ_Q	Borders
$[0, \psi_{P_S}]$	$\partial\Omega_P$, T_P^R, T_P^L, s_P^R
$[\psi_{P_S}, \psi_m]$	$\partial\Omega_P$, $I_{P_S}^R$, C_S, T_P^R, T_P^L, s_P^R
$[\psi_m, \psi_v]$	$I_{P_S}^R$, C_S, C_m^R, T_M^L, T_M^R, $s_{M_m}^R$, s_P^R
$[\psi_v, \psi_{O_1}]$	$I_{P_S}^R$, γ_v, C_S, T_V^L, T_M^L, T_M^R, $s_{M_m}^R$, s_P^R
$[\psi_{O_1}, \psi_{P_2}]$	γ_v, C_S, T_V^L, T_M^L, T_M^R, $s_{M_m}^R$, s_P^R
$[\psi_{P_2}, \psi_M]$	$I_{P_2}^R$, C_2, I_W^L, C_S, T_V^L, T_M^L, T_M^R, $s_{M_m}^R$
$[\psi_M, \psi_{O_2}]$	$I_{P_2}^R$, C_2, I_W^L, C_S, T_V^L, C_M^R, s_M^R, $s_{M_m}^R$
$[\psi_{O_2}, \psi_W]$	C_2, I_W^L, C_S, T_V^L, C_M^R, s_M^R, $s_{M_m}^R$
$[\psi_W, \psi_V]$	C_2, C_S, $T_{P'_N}^L$, T_V^L, C_M^R, s_M^R, $s_{M_m}^R$
$[\psi_V, \psi_{P'_N}]$	C_2, C_S, $T_{P'_N}^L$, γ_V, s_V^R, s_M^R, $s_{M_m}^R$
$[\psi_{P'_N}, \pi]$	C_2, C_S, C_N, $s_{P'_N}^R$, s_V^R, s_M^R

TABLE III: Ranges of ψ_Q and borders for which $\rho(\psi)$ must be compared to ρ_Q. Borders are ordered for increasing values of $\rho(\psi)$.

Extremal arcs	Regions
S	$I, I_c^H, IV_c^H, V_c^H, VI_c^H, XII, XIII$
T^L	II^H, V^H, IX, XI
T^R	VI^H
I^R	II^V, III, VII
I^L	$VIII, X$

TABLE IV: Extremal arcs characterizing the regions.

and involutes of circle I (see also [4] and [5]), are

$$\begin{aligned} T_Q^L: &\quad \rho = \rho_Q e^{\frac{(\psi_Q - \psi)}{\tan\phi}} \\ T_Q^R: &\quad \rho = \rho_Q e^{-\frac{(\psi_Q - \psi)}{\tan\phi}} \\ I_Q^L: &\quad \rho = \frac{R_b}{\cos\beta},\ \beta \text{ solution of } \psi - \psi_Q = \tan\beta - \beta \\ I_Q^R: &\quad \rho = \frac{R_b}{\cos\beta},\ \beta \text{ solution of } \psi - \psi_Q = -\tan\beta + \beta\,. \end{aligned} \tag{11}$$

The same does not occur in case of paths starting from regions characterized by S (i.e. Regions $I, I_c^H, IV_c^H, V_c^H, VI_c^H, XII, XIII$). From Regions I and I_c^H the straight line connects Q directly to P and in [17] a method to determine the direction towards P from these regions is provided. On the other hand, from points Q in the other regions we need to consider the border between the region in which Q lays and the following region crossed by the path. The intersection point between $\partial\Omega_Q$ and the considered border must be computed. For example, referring to Fig. 11 and Table IV, for a vehicle on Q in Region $XIII$, let us consider the intersection point between Ω_G (in particular the border C_Q^L) and C_N. The vehicle first reaches this point along a straight arc S from Q and then it crosses Region IX by following a spiral arc T^L until C_S is reached. Region $VIII$ is thus crossed along the involute arc I^L. Once C_2 is reached the vehicle first rotates on the spot and then it follows arc Z until it reaches P_2 where, after another rotation on the spot, it proceeds backward along the arc $I_{P_2}^R$ characterizing Region III until C_S. Finally the vehicle crosses Region VI^H along T^R (still moving backward) and once the border of Region I is reached it moves backward along the straight line toward P. On the other hand, from point Q in Region V_c^H, let us consider the intersection point between Ω_Q and $T_{M_m}^R$. After having reached this point by following a straight line S, the vehicle crosses Region II^H along a spiral arc T^L until T_P^R is reached. After a rotation on the spot it proceeds backward along the arc T_P^R (border between Regions II^H and VI^H) toward P.

To conclude this section, we will describe the path of the landmark in the image plane while the vehicle follows an infimum length path. Let us start from the extremal arcs. If the vehicle moves along a straight line S, also the landmark moves along a straight line passing through its initial position and the principal point of the image plane (cf. O_I in Fig. 12(a)). On the other hand, if the vehicle executes a rotation on the spot, the landmark moves along a conic curve (cf. Fig. 12(b)), see e.g. [18]. Finally, while the vehicle moves along a spiral or an involute arc, the landmark moves along the borders of the image plane. In particular, along the right or left borders in case of a left or right spirals (cf. Fig. 12(c)), along the left half or the right half upper (lower) borders in case of right or left involutes (cf. Fig. 12(d)).

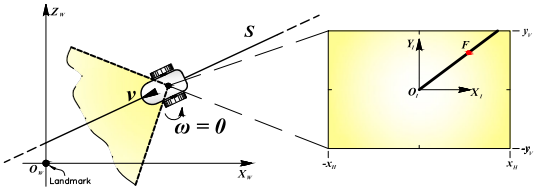

(a) Straight line path S.

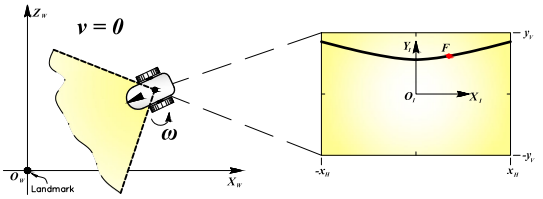

(b) Rotation on the spot $*$.

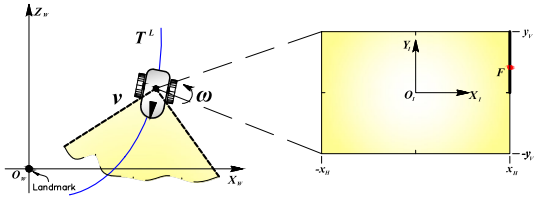

(c) Spiral arc T.

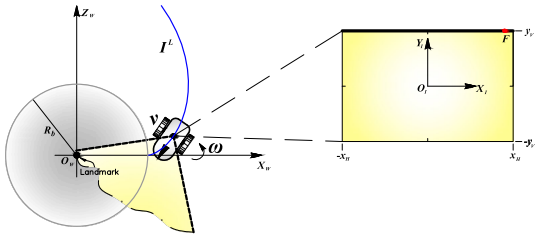

(d) Involute arc I.

Fig. 12: Paths of the landmark in the image plane.

Let us now assume that the vehicle is in Region $XIII$ aiming at the landmark. The path of the landmark in the image plane is represented in Fig. 13. The landmark has to first reach the right border of the image plane by following a conic curve, so that the vehicle is aligned to the straight line passing from the intersection point between C_Q^L and C_N, and then a straight line passing through the principal point (see [18] to determine the straight line to be followed) corresponding to arc S. Once the right border is reached, the vehicle is on C_N and the landmark follows the right border toward the upper (or lower) one (corresponding to arc T). Once the upper

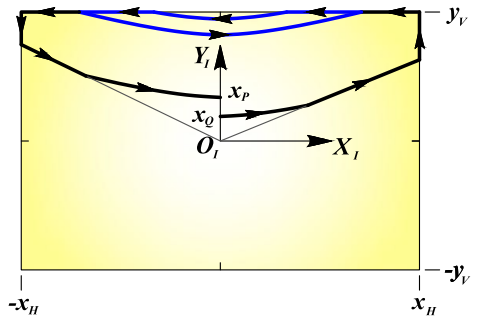

Fig. 13: The path of the landmark in the image plane along the infimum length path $S^{+}T^{L+} * I^{L+} * Z_{\varepsilon} * I^{R-}T^{R-}S^{-}$ of Region *XIII*. The subpath Z_{ε} is represented in blue.

(or lower) border is reached, the landmark is at the corner of the image plane and the vehicle is on C_S. The landmark proceeds by moving along the upper (lower) border until the vehicle reaches the circumference C_2 along arc I. The bearing angle is hence $\beta_{C_2} = \arccos(1/\sqrt{2})$. It is worth noting that the bearing angle is the only state variable that can be determined directly in the image plane: $\beta = \arctan\left(\frac{{}^{I}x}{\alpha_x}\right)$, where ${}^{I}x$ is the x coordinate of the landmark and α_x is a camera parameter (see also [18]). Hence, when the vehicle is following an involute it is possible, from the position of the landmark in the image plane, to determine when the vehicle is on circumference C_2. The extremal arc Z has now to be followed until point P_2 is reached. From a practical point of view, let us consider the arc Z_{ε} that corresponds to sequences of conics, segment of the left half upper (lower) border, conics and segment of the right half upper (lower) border (arcs $*I^R * I^L * I^R * \ldots$ in the motion plane, reported in blue in Fig. 13). At point P_2, the vehicle is on C_2 aligned to a right involute of circle I^R. As a consequence, the landmark is on the left half upper (lower) border and has to move along it until the left border of the image plane is reached. At this point the vehicle is on C_S. The landmark has to move now along the left border, toward the lower (upper) border of the camera. Once the border of Region I is reached, the landmark moves along a straight line through and toward the principal point until P is reached. To align the vehicle toward the landmark a final conic is followed.

VII. Conclusions and Future works

In this paper, the complete optimal synthesis of optimal (shortest) or ε–optimal paths (when the optimal path does not exist) has been obtained for a vehicle equipped with a sensor (e.g. a camera) with both vertical and horizontal bounds, which moves on a plane toward a desired configuration while maintaining a given landmark always in sight.

Future works on this subject are dedicated to translate the synthesis into stabilizing feedback control laws, extending to this work what it has been done in [17]. Another interesting problem is to consider different cost to be minimized, as e.g. time, energy, wheel rotations etc.. In [19] a first attempt to solve the minimum time problem has been done.

References

[1] F. A. Belo, P. Salaris, D. Fontanelli, and A. Bicchi, "A complete observability analysis of the planar bearing localization and mapping for visual servoing with known camera velocities," *International Journal Advanced Robotic Systems*, vol. 10, no. 197, 2013.

[2] P. Murrieri, D. Fontanelli, and A. Bicchi, "A hybrid-control approach to the parking problem of a wheeled vehicle using limited view-angle visual feedback," *International Journal of Robotics Research*, vol. 23, no. 4–5, pp. 437–448, April–May 2004.

[3] N. Gans and S. Hutchinson, "Stable visual servoing through hybrid switched system control," *IEEE Transactions on Robotics*, vol. 23, no. 3, pp. 530–540, June 2007.

[4] P. Salaris, D. Fontanelli, L. Pallottino, and A. Bicchi, "Shortest paths for a robot with nonholonomic and field-of-view constraints," *IEEE Transactions on Robotics*, vol. 26, no. 2, pp. 269–281, April 2010.

[5] P. Salaris, A. Cristofaro, L. Pallottino, and A. Bicchi, "Epsilon–optimal synthesis for vehicles with vertically bounded field-of-view," *Automatic Control, IEEE Transactions on*, vol. 60, no. 5, pp. 1204–1218, 2015.

[6] P. Salaris, L. Pallottino, and A. Bicchi, "Shortest paths for finned, winged, legged, and wheeled vehicles with side-looking sensors," *The International Journal of Robotics Research*, vol. 31, no. 8, pp. 997–1017, 2012.

[7] L. E. Dubins, "On curves of minimal length with a constraint on average curvature, and with prescribed initial and terminal positions and tangents," *American Journal of Mathematics*, pp. 457–516, 1957.

[8] T. Pecsvaradi, "Optimal horizontal guidance law for aircraft in the terminal area," *Automatic Control, IEEE Transactions on*, vol. 17, no. 6, pp. 763–772, Dec 1972.

[9] X. Bui, P. Souères, J.-D. Boissonnat, and J.-P. Laumond, "Shortest path synthesis for Dubins non–holonomic robots," in *IEEE International Conference on Robotics and Automation*, 1994, pp. 2–7.

[10] J. A. Reeds and L. A. Shepp, "Optimal paths for a car that goes both forwards and backwards," *Pacific Journal of Mathematics*, pp. 367–393, 1990.

[11] H. Sussmann and G. Tang, "Shortest paths for the reeds-shepp car: A worked out example of the use of geometric techniques in nonlinear optimal control," Department of Mathematics, Rutgers University, Tech. Rep., 1991.

[12] P. Souères and J. P. Laumond, "Shortest paths synthesis for a car-like robot," *IEEE Transaction on Automatic Control*, pp. 672–688, 1996.

[13] D. Balkcom and M. Mason, "Time-optimal trajectories for an omni-directional vehicle," *The International Journal of Robotics Research*, vol. 25, no. 10, pp. 985–999, 2006.

[14] H. Wang, Y. Chan, and P. Souères, "A geometric algorithm to compute time-optimal trajectories for a bidirectional steered robot," *IEEE Transaction on Robotics*, pp. 399–413, 2009.

[15] H. Chitsaz, S. M. LaValle, D. J. Balkcom, and M. Mason, "Minimum wheel-rotation for differential-drive mobile robots," *The International Journal of Robotics Research*, pp. 66–80, 2009.

[16] P. Salaris, A. Cristofaro, and L. Pallottino, "Additional material for: Epsilon–optimal synthesis for nonholonomic vehicles with limited field-of-view sensors," http://www.centropiaggio.unipi.it/sites/default/files/hvfov_additionalmaterial.pdf, 2015.

[17] P. Salaris, L. Pallottino, S. Hutchinson, and A. Bicchi, "From optimal planning to visual servoing with limited fov," in *Intelligent Robots and Systems, 2011. IROS 2011. IEEE/RSJ International Conference on*, 2011, pp. 2817–2824.

[18] P. Salaris, F. Belo, D. Fontanelli, L. Greco, and A. Bicchi, "Optimal paths in a constrained image plane for purely image-based parking," in *Intelligent Robots and Systems, 2008. IROS 2008. IEEE/RSJ International Conference on*, 2008, pp. 1673–1680.

[19] A. Cristofaro, P. Salaris, L. Pallottino, F. Giannoni, and A. Bicchi, "On time-optimal trajectories for differential drive vehicles with field-of-view constraints," in *53th IEEE Conference on Decision and Control*, 2014, pp. 2191–2197.

Paolo Salaris Paolo Salaris received the "Laurea" in Electrical Engineering in 2007 and the Doctoral degree in Robotics, Automation and Bioengineering in 2011 at the Research Center "E.Piaggio" of the University of Pisa. He has been Visiting Scholar at Beckman Institute for Advanced Science and Technology, University of Illinois, Urbana-Champaign in 2009. He has been a PostDoc at the Research Center "E.Piaggio" in Pisa (IT) from 2011 to 2013 and at LAAS-CNRS in Toulouse (FR) from February 2014 to July 2015. He is currently a Chargé de Recherche 2ème classe (CR2) at INRIA in Sophia Antipolis (FR). His main research interests within Robotics are in optimal motion planning, control for nonholonomic vehicles, visual servo control and motion segmentation and generation for humanoid robots.

Andrea Cristofaro has received the M.Sc. in Mathematics from University of Rome La Sapienza (Italy) in 2005 and the PhD in Information Science and Complex Systems from University of Camerino (Italy) in 2010. Between 2010 and 2013 he has been first with eMotion research team, INRIA Rhone-Alpes, Grenoble (France) and then with Department of Mathematics, University of Camerino (Italy). He is currently a post-doc researcher at the Department of Engineering Cybernetics, Norwegian University of Science and Technology and Center for Autonomous Marine Operations and Systems (AMOS), Trondheim (Norway). His research interests include: constrained and robust control, filtering and estimation methods, optimization, control allocation, autonomous vehicles, control of partial differential equations.

Lucia Pallottino received the "Laurea" degree in Mathematics from the University of Pisa in 1996, and the Ph.D. degree in Robotics and Industrial Automation degree from the University of Pisa in 2002. She has been Visiting Scholar in the Laboratory for Information and Decision Systems at MIT, Cambridge, MA and Visiting Researcher in the Mechanical and Aerospace Engineering Department at UCLA, Los Angeles, CA. She joined the Faculty of Engineering in the University of Pisa as an Assistant Professor in 2007. She currently is Associate Professor in Robotics. Her main research interests within Robotics are in optimal motion planning and control, planning and control of multi-agent systems and cooperating objects.